Electronic Supplementary Material (ESI) for Green Chemistry.

Solar-heating Thermocatalytic H_2 Production from Formic Acid by a MoS_2-Graphene-Nickel Foam Composite

Xianhua Bai,‡[a] Sipu Li,‡[a] Yufan Zhang,‡[a] Shilei Zhu,[b] Linjie Gao,*[a] Ridong Cong,*[a,c] Wei Yu,*[a,c] Shufang Wang,[a] Baolai Liang,[a] Yaguang Li*[a,c]

[a] *Hebei Key Lab of Optic-electronic Information and Materials, National and Local Joint Engineering Laboratory of New Energy Photoelectric Devices, The College of Physics Science and Technology, Institute of Life Science and Green Development, Hebei University, Baoding, 071002, China.*

[b] *Department of Electronics and Optical Engineering, Army Engineering University, Shijiazhuang 050003, China.*

[c] *State Key Laboratory of Photovoltaic Materials & Technology, Yingli Solar, Baoding 071051, China.*

Correspondence and requests for materials should be addressed to L.J. Gao (LinjieGao@hotmail.com), R.D. Cong (congrd@126.com), W. Yu (yuwei@hbu.edu.cn), Y.G. Li (liyaguang@hbu.edu.cn).

‡ These authors contributed equally.

Experimental Section

1.1 Chemicals

The hydrochloric acid, formic acid (FA), and sodium format (SF) were purchased from Kemel Chemical industry Co., Ltd. and were directly used without further treatment. The deionized water was produced by our laboratory.

1.2 The preparation of Cu_2Se based device

The SP-0707AS magnetron sputtering was used to deposit Cu_2Se film under vacuum pressure lower than 6.8×10^{-3} Pa. Cu_2Se and Cu were used as targets; the working gas was Ar with 99.9 % purity. The bases was a glass tube with 450 mm length and 35 mm of diameter. Before the deposition process, the bases were washing with deionized water, acetone, ethanol subsequently.

For the synthesis of device, the deposition of Cu substrate and Cu_2Se film on glass tube was first using glow-discharge to clean glass tube, then depositing Cu layer by Cu target and Cu_2Se film by Cu_2Se target orderly, finally taking out the sample after passive cooling. Specific parameters: the power was 5.0 KW, the sputtering pressure was 9.2×10^{-2} Pa, the sputtering time for Cu layer, Cu_2Se film was 13 min, 3 min, respectively. The followed glass vacuum layer was provided by Hebei scientist research experimental and equipment trade Co., Ltd. with 2.9×10^{-3} Pa of pressure.

1.3 Catalysts preparation

1. Treatment of Ni foam.

The Ni foam was soaked in 1 wt% HCl solution for 15min, then ultrasonic cleaned in deionized water for 5min, and repeated three times to remove residual chemicals. The washed Ni foam was dried in a vacuum oven for 2h at 80 °C.

2. Preparation of Ni/graphene (Ni/G) support.

Graphene was deposited on Ni foam to serve as the support under CH_4 atmosphere. The dried Ni foam was sealed in a quartz tube to grow graphene, 1000 sccm Ar flow was added for 15min to remove extra air. Mix gas (500 sccm Ar and 200 sccm H_2) was added into the quartz tube, then heated to 950-1020 °C and kept for 30min to remove the native oxide layer on the foam surface. Followed by the heating procedure, 2-5 sccm CH_4 gas flow was added and reacted for 5 min. After the reaction, stopped the CH_4 gas flow and added the mixed flow (500 sccm Ar and 200 sccm H_2) into the tube until it was naturally cooled down to room temperature. Finally, the Ni/graphene (Ni/G) support was obtained.

3. Preparation of Ni/G/MoS_2.

The as-prepared Ni/G was used as substrate and MoS_2 was grown on it by magnetron Sputtering. For a typical procedure, the Ni/G support was placed into a Magnetron Sputtering reaction chamber and vacuumed below $5*10^{-4}$ Pa, then adjusted the chamber pressure to 2 Pa by mix gas of Ar and H_2 (H_2 volume ratio was 0.5-10%). After heating the sample holder to 650 °C, opened the sputtering power (70 W) for 60 min to ablate the MoS_2 target. The sample was naturally cooled down to room temperature under the reaction atmosphere. Finally, a layered-petal-like Ni/G/MoS_2 sample was obtained.

1.4 Characterizations of Catalysts

The crystal structure of prepared samples was studied by the powder X-ray diffraction (XRD), which was performed on a Bede D1 system operated at 20 kV and 30 mA with Cu Kα radiation (λ=1.5406Å). The scanning electron microscopy (SEM, FEI Nova NanoSEM450) and transmission electron microscopy (TEM, JEOL 2100) were used to identify the morphology of the samples. Raman spectra were recorded on a HORIBA Raman spectrometer, with an excitation laser wavelength of 532 nm. The X-ray photoelectron spectra (XPS) were recorded on a Thermo ESCALAB-250Xi spectrometer with an amonochromatic Al Kα radiation source (1486.6 eV). The binding energies determined by XPS were corrected by referring to the adventitious carbon peak (284.8eV) for each sample. Zennium_Pro (Zahner, Germany) was an electrochemical workstation. The ultraviolet-visible-infrared absorption spectrum (UV-vis-IR) and IR emission were tested by Hitachi Limited U4100 (Japan) and

FTIR spectrometer (Bruker, VERTEX 70 FT-IR).The thermal conductivity were tested by thin film thermal conductivity meter (Linseis TF-LFA). The temperature of catalysts in device under different light intensity was tested by a thermometer (SM6806A).

1.5 First principle calculations

We have employed the Vienna Ab Initio Package (VASP)[1, 2] to perform all the density functional theory (DFT) calculations within the generalized gradient approximation (GGA) using the PBE formulation.[3] We have chosen the projected augmented wave (PAW) potentials to describe the ionic cores and take valence electrons into account using a plane wave basis set with a kinetic energy cutoff of 400 eV. Partial occupancies of the Kohn−Sham orbitals were allowed using the Gaussian smearing method and a width of 0.05 eV. The electronic energy was considered self-consistent when the energy change was smaller than 10^{-5} eV. A geometry optimization was considered convergent when the force change was smaller than 0.02 eV/Å. Grimme's DFT-D3 methodology[4] was used to describe the dispersion interactions.

We used MoS_2 (002) facet as the model. The equilibrium lattice constant of hexagonal MoS_2 unit cell separated by a vacuum layer in the depth of 30 Å was optimized, when using a 15×15×1 Monkhorst-Pack k-point grid for Brillouin zone sampling. We then used it to construct a MoS_2 model with *p*(7x7x3) periodicity in the x, y, z directions by vacuum depth of 30 Å in order to separate the surface slab from its periodic duplicates. During structural optimizations, the gamma point in the Brillouin zone was used for k-point sampling, and all atoms were allowed to relax.

The adsorption energy (E_{ads}) of adsorbate A was defined as

$E_{ads} = E_{A/surf} – E_{surf} - E_{A(g)}$

where $E_{A/surf}$, E_{surf} and $E_{A(g)}$ are the energy of adsorbate A adsorbed on the surface, the energy of clean surface, and the energy of isolated A molecule in a cubic periodic box with a side length of 20 Å and a 1×1×1 Monkhorst-Pack k-point grid for Brillouin zone sampling, respectively.

1.6 Thermocatalytic test

Typically, 0.5 mL distilled water and 10 mg fresh (20 mm*40 mm *1.6mm) prepared catalysts were mixed into a two-necked round-bottom flask (25 mL). One of the necks was linked to a gas burette, and the other was reserved by adding 0.5 mL FA-SF (1.25 mmol FA and 3.75 mmol SF) mixed solution. The dehydrogenation reaction was started as the FA-SF mixed solution was poured into the above round-bottom reaction flask under vigorously stirring. A thermostatic water bath was used to adjust reaction temperature. The product gas flow was carried out by 10 sccm Ar and tested by gas chromatography (GC) 7890A equipped with FID and TCD detectors. The results were showed in Fig. 2.

1.7 Solar-heating thermocatalytic catalytic activity

Solar-heating thermocatalytic was realized by using our Cu_2Se based device with 50 mg of catalysts. The laboratory light source used for the soalr-heating test is a Xenon lamp (HP-2-4000), and the light intensity can be tuned automatically. The Ni/G/MoS_2 catalyst was filled in our homemade device, and the device was exposed to sunlight irradiation. The temperature change of catalysts under different light intensity was tested by a thermometer (SM6806A), which was inserted into the Ni/G/MoS_2. The feed gas with 100 sccm of flow rate was passed through the FA-SF (mole ratio FA:SF=1:3) mixed solution into the reactor. We first removed CO_2 in the produced gas through NaOH solution (5 M), and a flowmeter (MV-192-H2, Bronkhorst) was used to measure the flow rate and the gas composition was tested by gas chromatography (GC) 7890A equipped with FID and TCD detectors.

The H_2 production rate (mmol g^{-1} h^{-1}) is calculated by the following formula:

$$H_2\ production\ rate = \frac{60 * V * S}{24.5 * m_{catalyst}}$$

V: The flow rate of gas, unit ml/min (sccm);

S: The H_2 concentration in outlet gas, tested by GC.

$m_{catalyst}$: The mass of catalysts. unit g.

Tab. S1 Comparison solar-heating thermocatalytic catalytic dehydrogenation of FA by Ni/G/MoS_2 with other photocatalyst.

Photocatalyst	Light source	H_2 rate ($mmol\cdot g^{-1}\cdot h^{-1}$)	Selectivity	Reference
Ni/G/MoS_2	0.6 Sun	982	100%	This work
Ru-CdS	Xenon lamp	0.54	none	5
Rh-N: TiO_2	Xenon lamp	0.746	98%	6
Pd/C_3N_4	Xenon lamp	53.4	none	7
Co^{2+}/CdS QDs	Xenon lamp	116 ± 14	99.4 ± 0.1%	8
$Au_{0.75}Pd$ /TiO_2	1 Sun	17.7	99.5%	9
CdS/CoP@RGO	Xenon lamp	182± 12.5	99.5%	10
MoS_2/$Zn_3In_2S_6$	Xenon lamp	0.7425	none	11
Pt/g-C_3N_4	0.7 sun	1.59	none	12
FeP@CdS NRs	Xenon lamp	278	none	13
CoPSA-CdS NRs	Xenon lamp	102.9	none	14
Fe salen/CdS	Xenon lamp	150	none	15

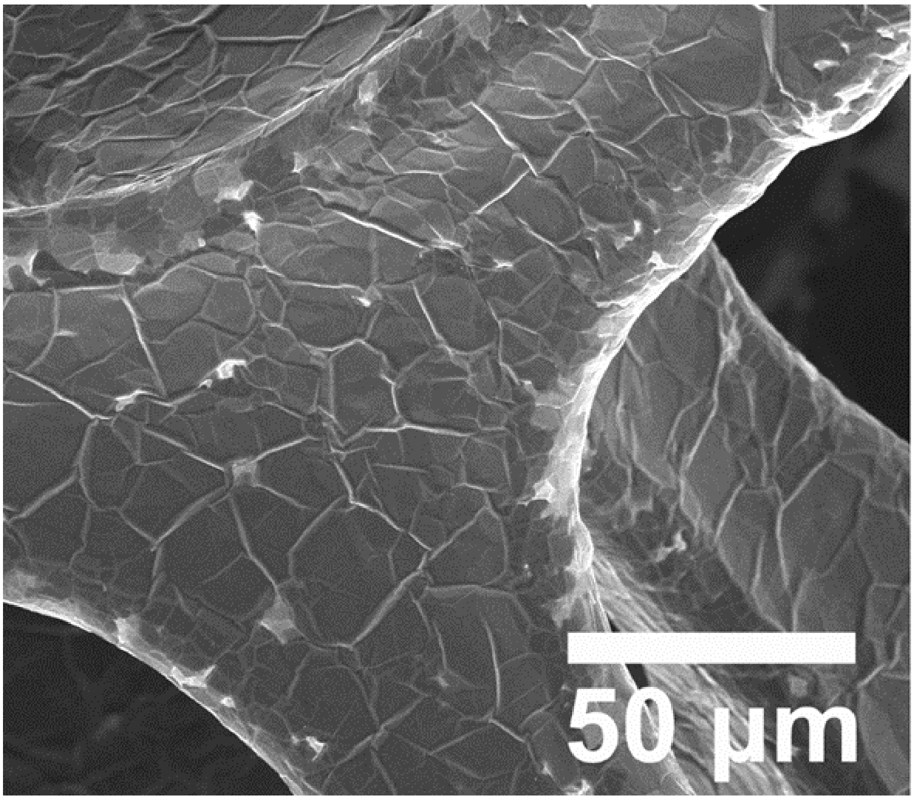

Fig. S1 SEM image of Ni foam.

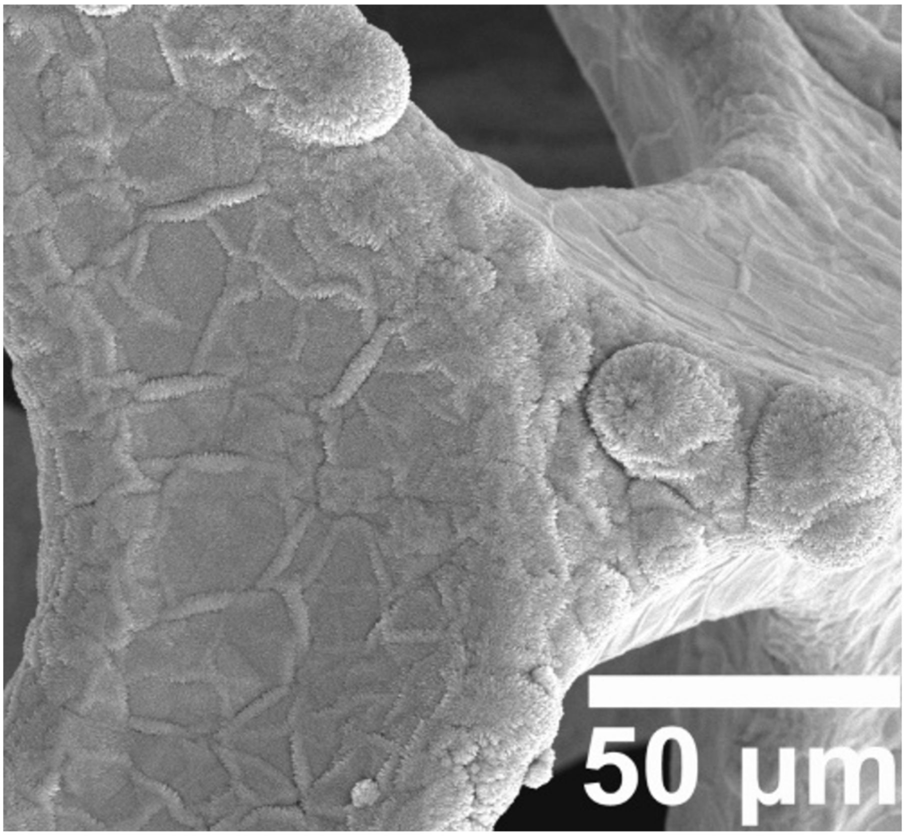

Fig. S2 SEM image of Ni/G/MoS_2.

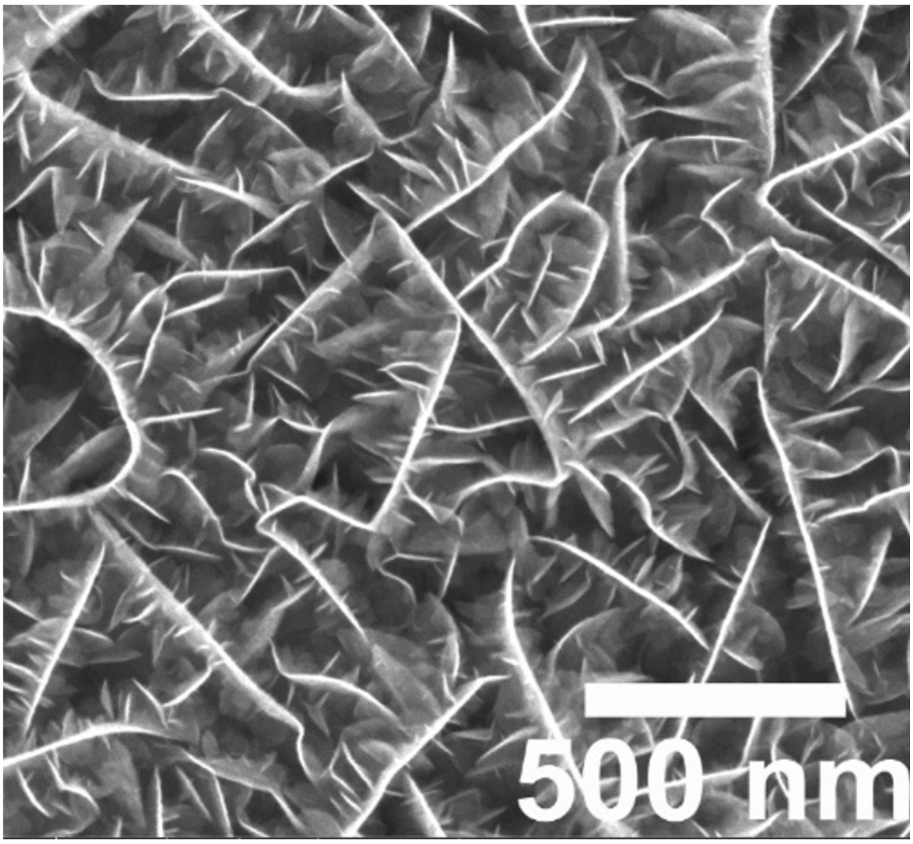

Fig. S3 High-magnification SEM image of Ni/G/MoS_2

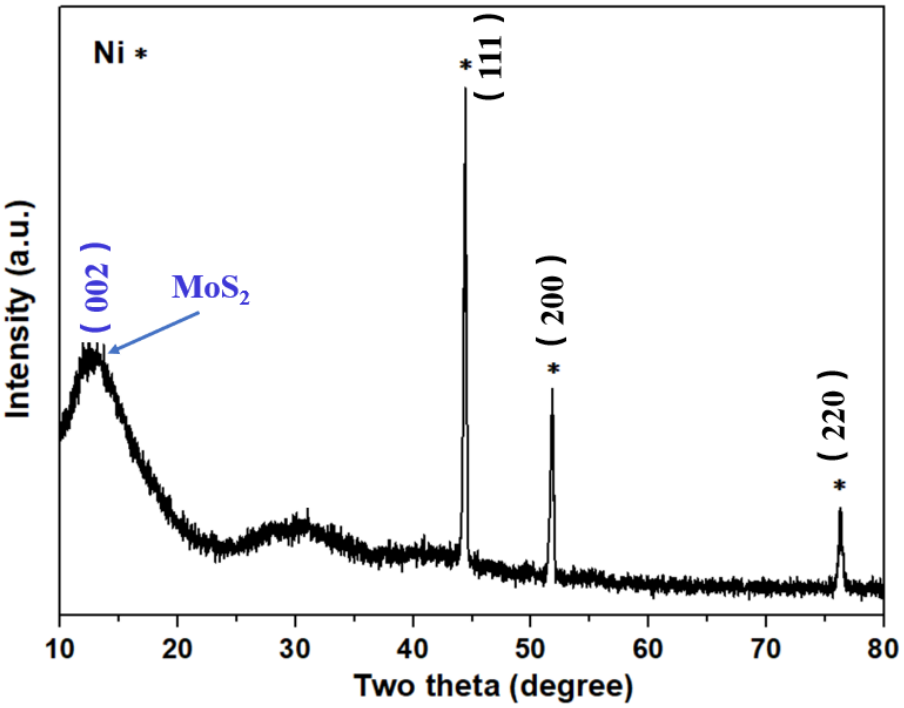

Fig. S4 The XRD pattern of the prepared Ni/G/MoS_2.

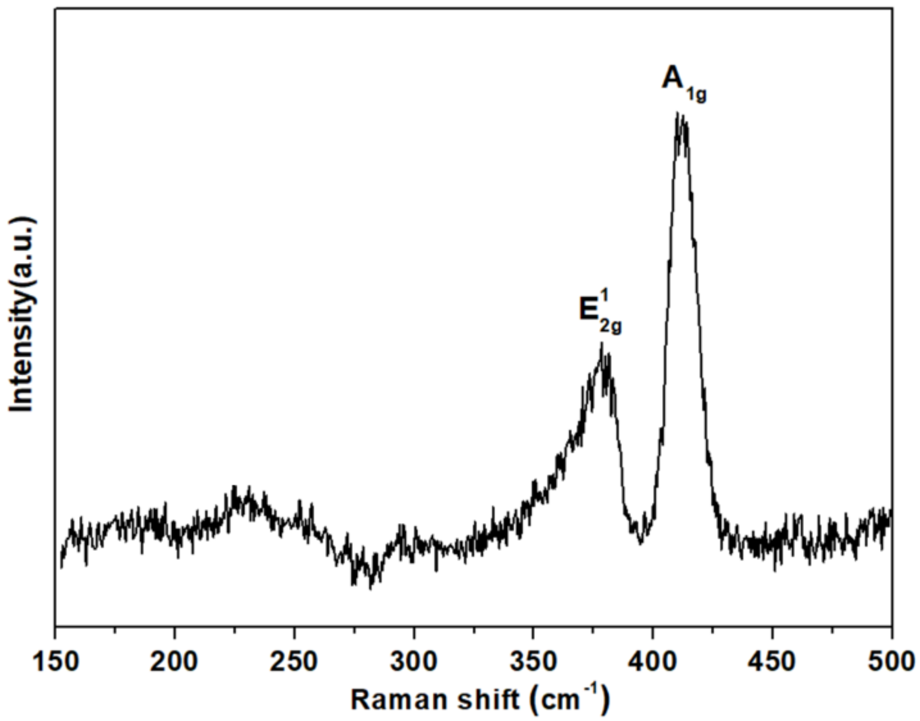

Fig. S5 Raman spectra of the Ni/G/MoS_2 sample.

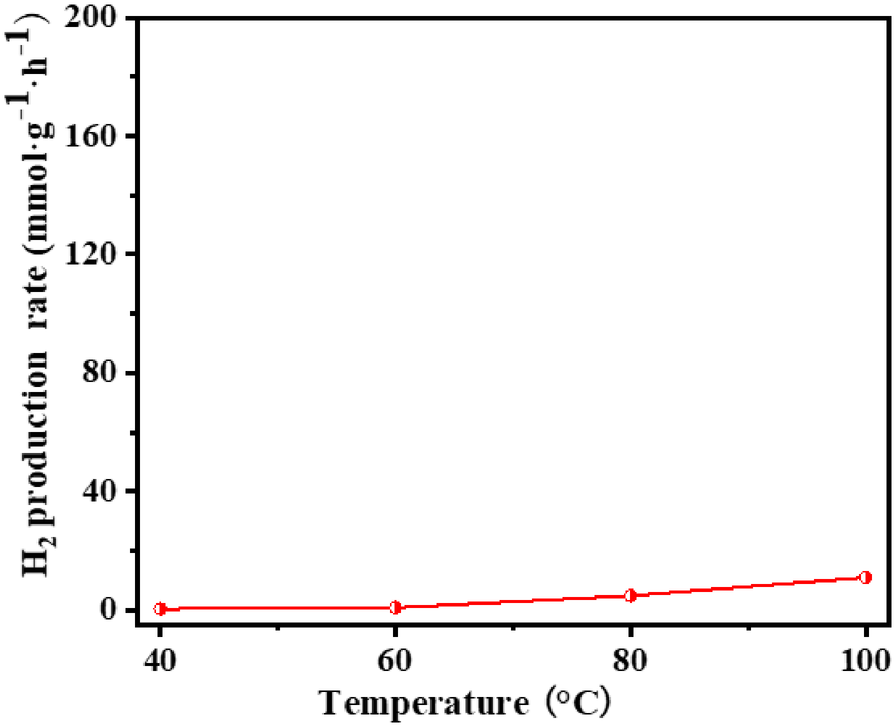

Fig. S6 Thermocatalytic H_2 production from formic acid for the Ni/G.

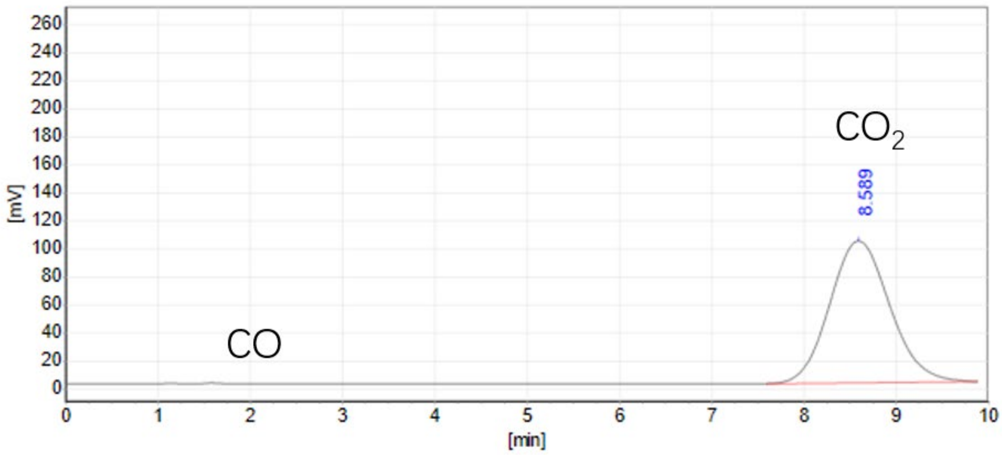

Fig. S7 The FID spectrum from the thermocatalytic H_2 production from formic acid for Ni/G/MoS_2 catalysts.

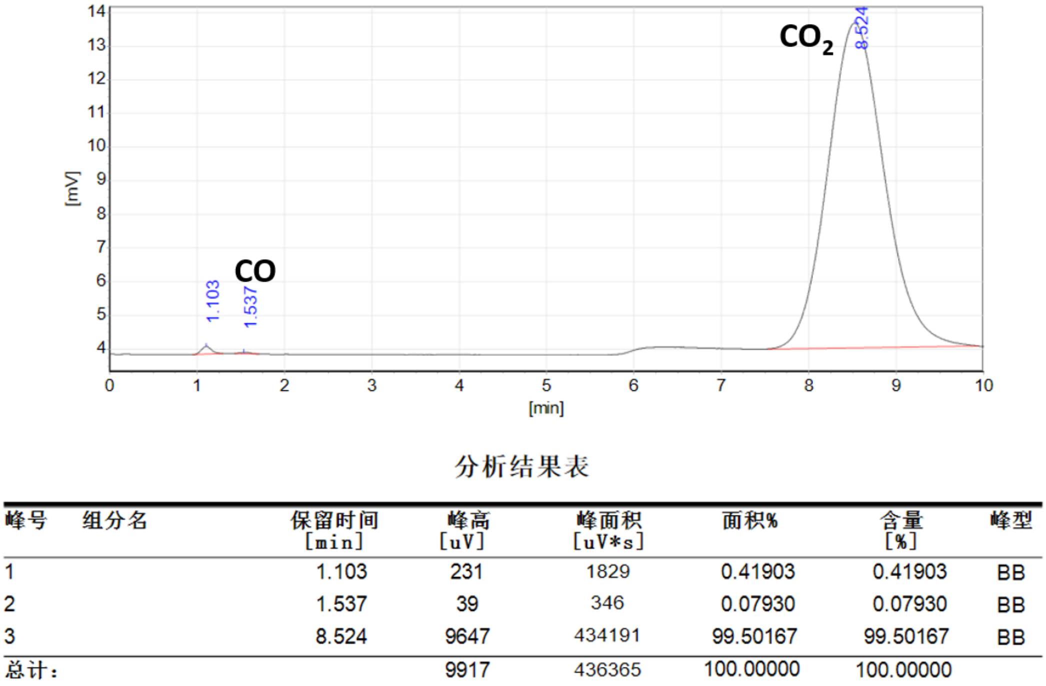

分析结果表

峰号	组分名	保留时间 [min]	峰高 [uV]	峰面积 [uV*s]	面积%	含量 [%]	峰型
1		1.103	231	1829	0.41903	0.41903	BB
2		1.537	39	346	0.07930	0.07930	BB
3		8.524	9647	434191	99.50167	99.50167	BB
总计：			9917	436365	100.00000	100.00000	

Fig. S8 The FID curve of mixture with 0.1 ppm of CO.

As shown in Fig. S8, we tested the mixed gas containing 0.1 ppm of CO, which can be identified in our GC (the area of 0.1 ppm CO equals to 320, and the peak in 1.103min was a fluctuation due to the presence of water vapor). Compared with Fig. S7, it indicates that the detector has an ultra-high CO detection limit.

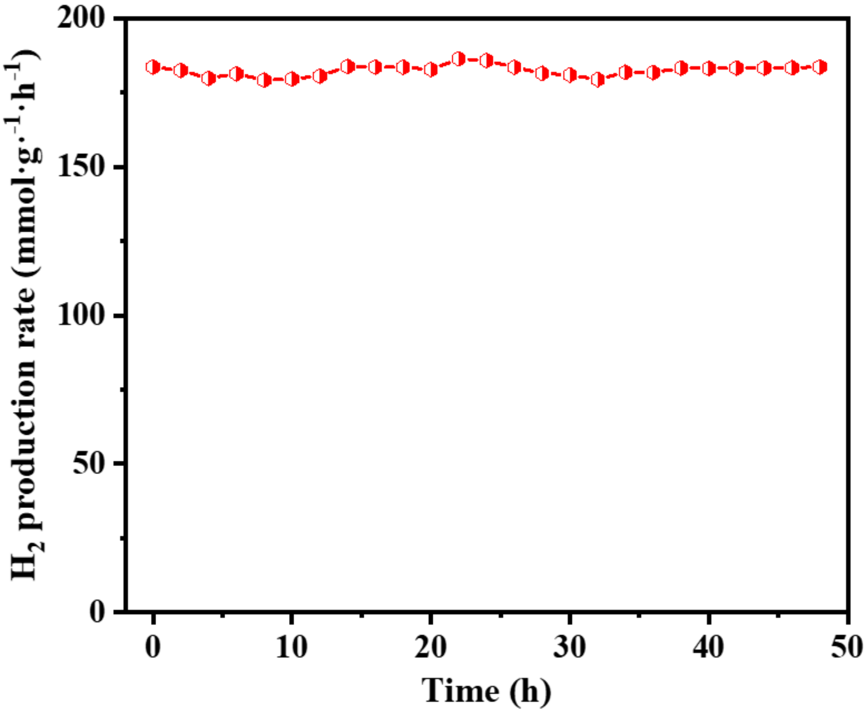

Fig. S9 Thermocatalytic stability of H_2 production from formic acid through Ni/G/MoS_2 under 100 °C during 48h.

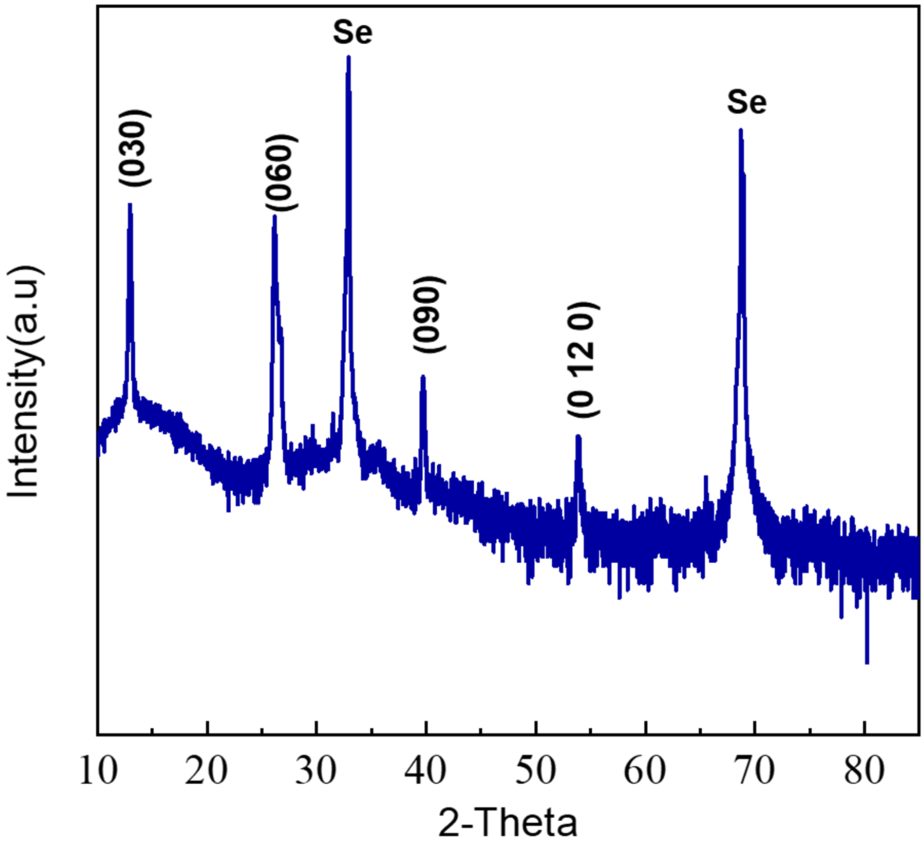

Fig. S10 The XRD pattern of Cu_2Se.

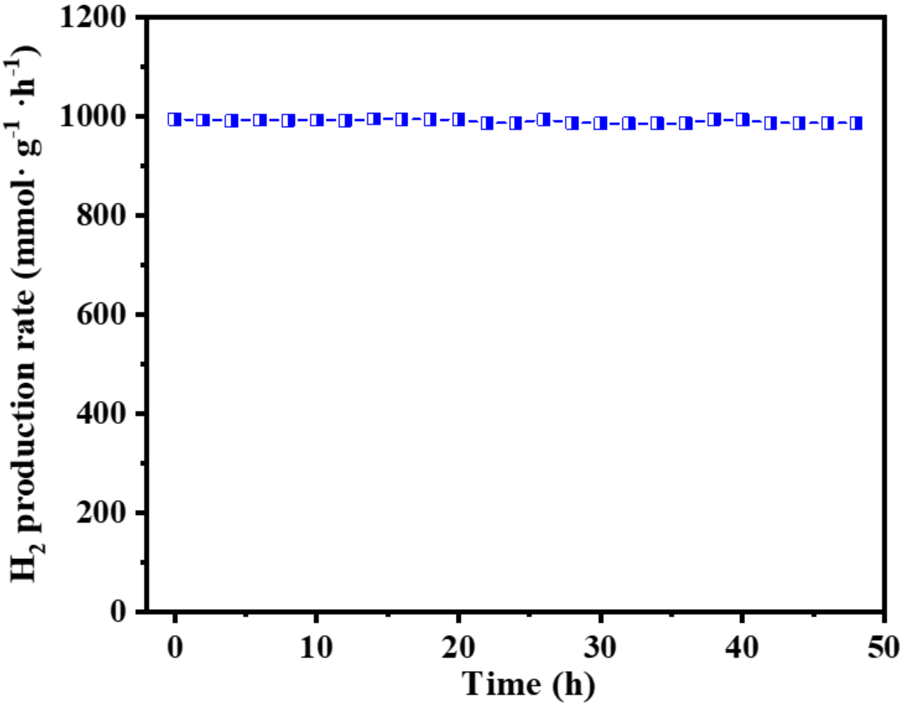

Fig. S11 Solar-heating stability of H_2 production from formic acid through Ni/G/MoS_2 under 0.6 Sun irradiation during 48h.

References

1. G. Kresse and J. Furthmüller, *Computational Materials Science*, 1996, **6**, 15-50.
2. G. Kresse and J. Furthmüller, *Physical Review B*, 1996, **54**, 11169-11186.
3. J. P. Perdew, K. Burke and M. Ernzerhof, *Physical Review Letters*, 1996, **77**, 3865-3868.
4. S. Grimme, J. Antony, S. Ehrlich and H. Krieg, *The Journal of Chemical Physics*, 2010, **132**, 154104.
5. Y. J. Zhang, L. Zhang and S. Li, *International Journal of Hydrogen Energy*, 2010, **35**, 438-444.
6. G. Halasi, G. Schubert and F. Solymosi, *Catalysis Letters*, 2011, **142**.
7. Y.-Y. Cai, X.-H. Li, Y.-N. Zhang, X. Wei, K.-X. Wang and J.-S. Chen, *Angewandte Chemie International Edition*, 2013, **52**, 11822-11825.
8. M. F. Kuehnel, D. W. Wakerley, K. L. Orchard and E. Reisner, *Angewandte Chemie International Edition*, 2015, **54**, 9627-9631.
9. Z. Zhang, S.-W. Cao, Y. Liao and C. Xue, *Applied Catalysis B: Environmental*, 2015, **162**, 204-209.
10. S. Cao, Y. Chen, H. Wang, J. Chen, X. Shi, H. Li, P. Cheng, X. Liu, M. Liu and L. Piao, *Joule*, 2018, **2**, 549-557.
11. S. Zhang, S. Duan, G. Chen, S. Meng, X. Zheng, Y. Fan, X. Fu and S. Chen, *Chinese Journal of Catalysis*, 2021, **42**, 193-204.
12. J. Wang, X. Wang, L. Qiu, H. Wang, L. Duan, Z. Kang and J. Liu, *Nanotechnology*, 2021, **32**, 275404.
13. T. Wang, L. Yang, D. Jiang, H. Cao, A. C. Minja and P. Du, *ACS Applied Materials & Interfaces*, 2021, **13**, 23751-23759.

14. P. Zhou, Q. Zhang, Z. Xu, Q. Shang, L. Wang, Y. Chao, Y. Li, H. Chen, F. Lv, Q. Zhang, L. Gu and S. Guo, *Advanced Materials*, 2020, **32**, 1904249.
15. R. M. Irfan, T. Wang, D. Jiang, Q. Yue, L. Zhang, H. Cao, Y. Pan and P. Du, *Angewandte Chemie*, 2020, **132**.